The RNA-Bound Conformation of Neamine as Determined by Transferred NOE Experiments

Richard Szilaghi, Syed Shahzad-ul-Hussan, and Thomas Weimar*[a]

The $tRNA^{Phe}$-bound conformation of the aminoglycoside neamine, a member of the neomycin B family, has been investigated by transferred NOE experiments in aqueous solution. This is the first time that the bioactive conformation of an RNA-bound aminoglycoside has been determined by this method. In buffers without divalent Mg^{2+} ions, a high degree of electrostatically driven unspecific binding of aminoglycosides to the RNA was observed. Careful optimization of experimental conditions yielded buffer conditions optimized for cryo-probe NMR experiments. In particular, addition of Mg^{2+} ions to the solutions was necessary to reduce the amount of unspecific binding as monitored by one-dimensional NMR and surface plasmon resonance experiments. CD spectroscopy was used to probe the effect of aminoglycosides and buffer conditions on the double helical content of $tRNA^{Phe}$. Finally the $tRNA^{Phe}$-bound conformation of neamine was determined by trNOE build-up curves and compared with the previously reported crystal structure of neomycin B complexed to this RNA. Although the aminoglycoside in the crystal structure contains several configurational errors, the overall shape of the crystallographically determined RNA-bound structure is identical to the RNA-bound conformation defined by the NMR experiments. Therefore, the crystal structure has been refined by trNOE data. This is particularly important in the context of aminoglycosides being discussed as lead structures for the development of new anti-RNA drugs.

Introduction

Food production and healthcare systems worldwide are permanently threatened by microorganisms and viruses, most of them requiring RNA structures in various forms in order to function. Since RNA is structurally and functionally much more diverse than DNA, RNA structures are very promising targets for the development of new antibacterial, antiviral, and antifungal agents.[1] Aminoglycosides are a class of small molecules known to modify the biological function of many RNA structures, for example, bacterial rRNA,[2] group I introns,[3] and the hammerhead[4] and hepatitis delta virus ribozymes.[5] Aminoglycosides have also been shown to inhibit the interaction of the Rev protein[6] and the Tat peptide[7] with their viral RNA targets, whilst inhibition of the aminoacylation of yeast $tRNA^{Asp}$ by tobramycin[8] and of *E. coli* $tRNA^{Phe}$ by neomycin B have recently been demonstrated.[9] The potential to use aminoglycosides as scaffolds for the design of new specific anti-RNA drugs is therefore evident.

NMR and crystallographic studies have shown that aminoglycosides can bind to very specific binding sites on RNA structures,[10] and in this way interfere with the biological function of the target. The structure-based drug design of new anti-RNA drugs requires comprehensive understanding of the target system at atomic resolutions, but crystal structures sometimes do not correctly define small molecules bound to macromolecules. An example is the recently published crystal structure of $tRNA^{Phe}$ from yeast in complexation with neomycin B (see Scheme 1), which features several configurational errors in the aminoglycoside.[9] Out of 19 chiral carbon atoms, only eight have the correct absolute configuration. Since atoms C1 in the glucopyranose (G) and the idopyranose (I) unit belong among these wrongly configured carbon atoms, the 2,6-dideoxy-2,6-diamino-α-D-glucopyranose unit (G) is β-configured and the 2,6-dideoxy-2,6-diamino-β-L-idopyranose unit (I) is α-configured in the crystal structure of $tRNA^{Phe}$-bound neomycin B. The reason for these errors might be wrong configurational input caused by the relatively low resolution (2.6 Å) and high crystallographic B-factors, especially around the aminoglycoside binding site. Here NMR spectroscopy offers a complementary source of structural data through transferred NOE (trNOE) experiments, which can define the bioactive conformation of a small ligand bound to a macromo-

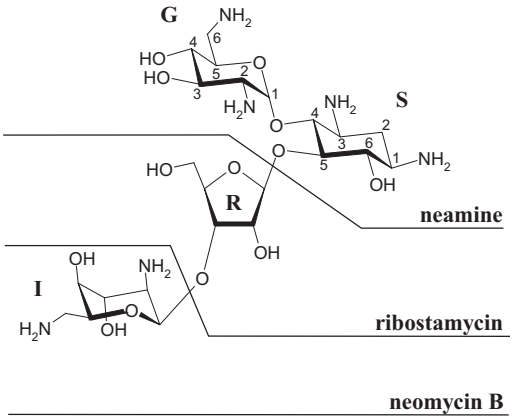

Scheme 1. Schematic representation of neomycin A, ribostamycin, and neamine. The numbering of the carbon atoms in the 2,6-dideoxy-2,6-diamino-glucopyranose (G) and 2-deoxystreptamine ring (S) is indicated. R indicates the ribose and I the 2,6-dideoxy-2,6-diaminoidopyranose.

[a] *Dipl.-Chem. R. Szilaghi,[+] S. Shahzad-ul-Hussan,[+] Dr. T. Weimar*
Universität zu Lübeck, Institut für Chemie
Ratzeburger Allee 160, 23538 Lübeck (Germany)
Fax: (+49) 451-500-4241
E-mail: thomas.weimar@chemie.uni-luebeck.de
[+] *These authors contributed equally to this work.*

  DOI: 10.1002/cbic.200400363

lecule in aqueous solution.[11] This experimental approach has been used by several groups to study small ligand molecules bound to proteins. Interestingly, though, RNA structures have not been subjected to this technique very often; to the best of our knowledge there are only a few reports in which trNOE experiments have been used to investigate complexes of antibiotics with complete ribosomes or their subunits.[12] TrNOE experiments with complexes of smaller RNA structures and effector molecules, especially aminoglycosides, have yet to be reported.

In the course of a research project intended to characterize interactions between RNA and small ligand effectors, we were aiming to define the RNA-bound conformations of aminoglycosides by trNOE experiments. Since the described $tRNA^{Phe}$ is of comparable size to many other potential target RNAs, we used this $tRNA^{Phe}$ in complexation with neomycin B and its derivatives to evaluate whether trNOE experiments in general would be applicable to RNA-bound aminoglycosides. Here we report the $tRNA^{Phe}$-bound conformation of neamine, the component of neomycin B displaying most of the contacts to $tRNA^{Phe}$ in the crystal structure.

Results and Discussion

TrNOE experiments require a concentration of the ligand molecule in excess (usually between ten- and 20-fold) over the biomacromolecule. While performing NMR experiments with RNA/aminoglycoside mixtures at 1:20 ratios and fairly high concentrations (200 μM $tRNA^{Phe}$, 4 mM ribostamycin) we found that the resonances of the aminoglycosides were considerably broadened, suggesting intense contacts and/or long residence times of the aminoglycoside in the RNA-bound state (Figure 1). Precipitation was observed in these samples, as has been described previously.[13] The linewidths of the aminoglycoside resonances could be narrowed considerably simply by diluting the solution by a factor of twenty with buffer. As pK_a values of aminoglycoside amino functions are in a range between ≈6 and 9,[9,14] aminoglycosides can be regarded as oligovalent cationic molecules at physiological pH values. With polyvalent anionic RNA, electrostatic interactions account for strong attraction between these two types of molecules. Especially at high concentrations, these electrostatic interactions seem to force many aminoglycoside molecules to bind to the RNA and to form aggregates. In the context of defining aminoglycosides bound to a specific binding site on the RNA, this additional, electrostatically forced, binding of aminoglycosides was of course undesired and had to be avoided.

In vivo, RNA has different counterions, including Mg^{2+}, Ca^{2+}, and NH_4^+, together with polyamines such as spermine and spermidine.[15] The three-dimensional structure of RNAs are particularly strongly stabilized by the divalent ions, and it has been demonstrated that up to 25 Mg^{2+} ions can bind in an electrostatically driven fashion to a single $tRNA^{Phe}$.[16] Polyamines such as aminoglycosides compete with the divalent metal ions for the cation-binding sites on RNA. While working in fairly concentrated solutions we tried to keep a balance between RNA, counterions, and the aminoglycoside in the buffer

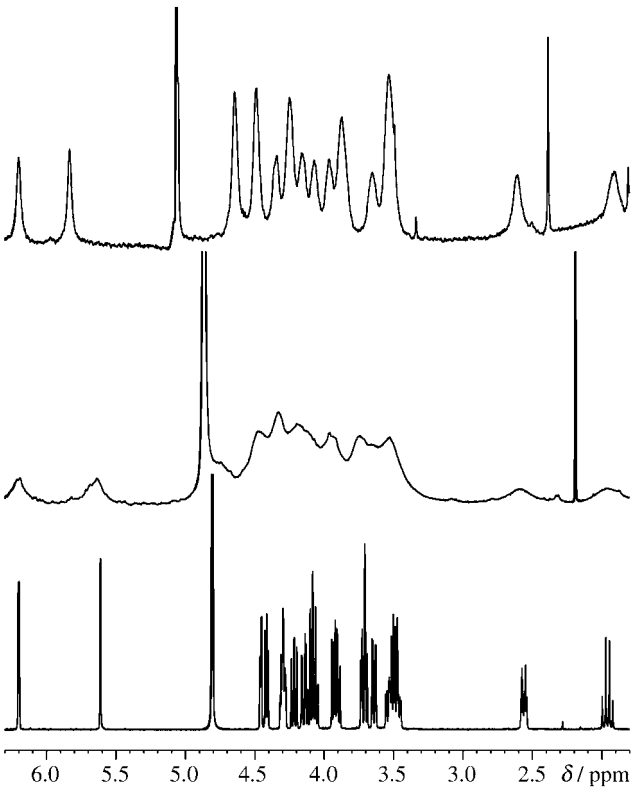

Figure 1. One-dimensional NMR spectra (500 MHz) of free ribostamycin (bottom), ribostamycin with $tRNA^{Phe}$ (≈0.2 mM $tRNA^{Phe}$, 4 mM ribostamycin) (middle), and a 20-fold diluted solution of this mixture (≈10 μM $tRNA^{Phe}$, 200 μM ribostamycin (top) in D_2O phosphate buffer in the absence of Mg^{2+} ions. In the more concentrated sample the ribostamycin resonances are very broad, indicating strong binding to the RNA. Precipitation was especially evident in this sample.

system, and therefore added $MgCl_2$ to mixtures of aminoglycosides and $tRNA^{Phe}$. The resulting one-dimensional NMR spectra are shown in Figure 2. As can be seen, the linewidths of aminoglycoside resonances in mixtures with $tRNA^{Phe}$ were consid-

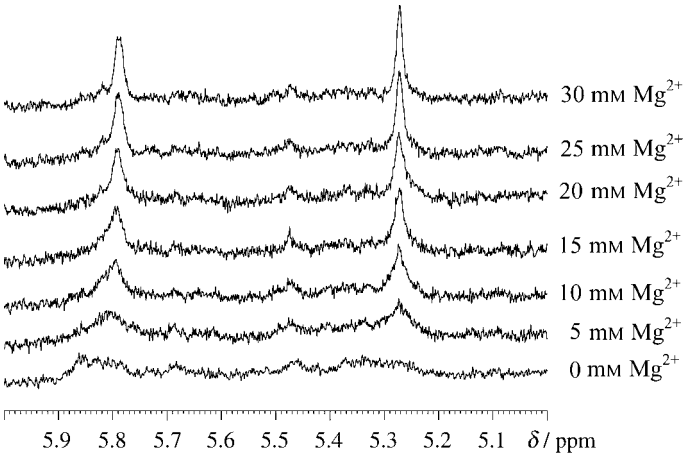

Figure 2. One-dimensional NMR spectra (500 MHz) of a $MgCl_2$ titration of a sample containing 250 μM ribostamycin and 16.6 μM $tRNA^{Phe}$ in deuterated Tris buffer. Only the region of the anomeric protons is shown. Mg^{2+} ions displace the bound aminoglycoside.

erably narrowed by addition of Mg^{2+}, indicating that Mg^{2+} was displacing aminoglycosides from the tRNA. Surface plasmon resonance experiments with immobilized $tRNA^{Phe}$ (Figure 3) were used to verify these results. In these experiments different concentrations of aminoglycosides were

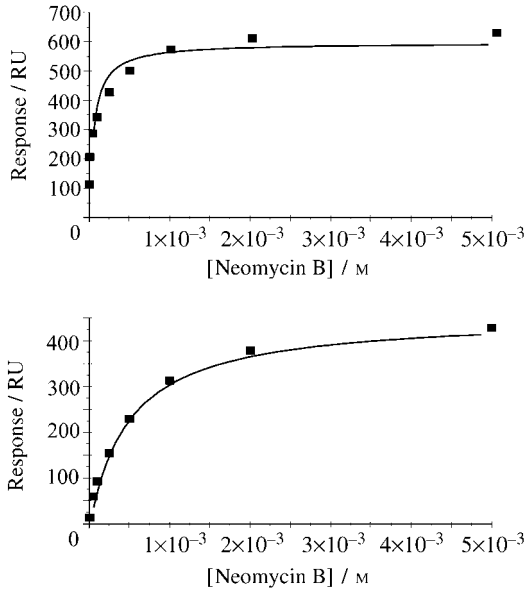

Figure 3. Binding isotherms from SPR experiments. Top: Tris buffer in the absence of $MgCl_2$. Bottom: Tris buffer with $MgCl_2$ (30 mM).

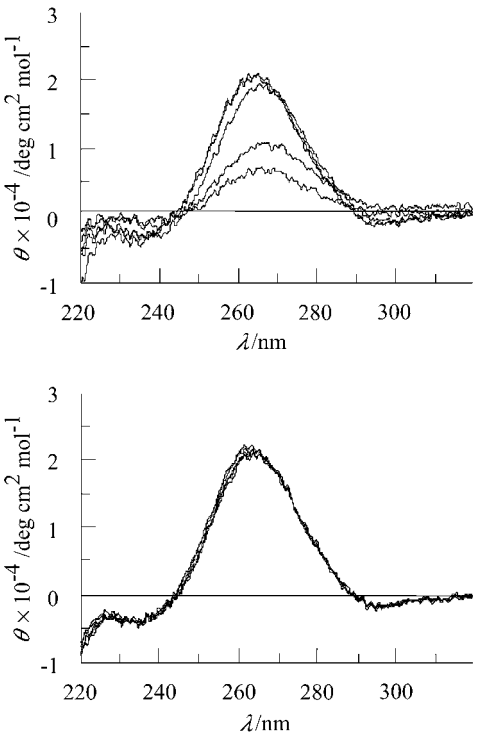

Figure 4. CD spectra of $tRNA^{Phe}$ (8 μM) in Tris buffer (40 mM, 20 mM NaCl, pH 7.2) and neomycin B concentrations of 0, 8, 120, 200, and 400 μM without (top) and with (bottom) Mg^{2+} (30 mM).

passed over a sensor chip surface with immobilized $tRNA^{Phe}$ and the equilibrium response was fitted to a binding isotherm. Without Mg^{2+} ions in the buffer, the experimental data were not in accordance with a binding model having a single binding site. Only binding models with more than one binding site and different affinities could reproduce the experimental data (not shown). This changed when Mg^{2+} was added to the buffer. Less binding occurred in the presence of the divalent ions, and the equilibrium data now fitted a model with a single binding site.

To improve buffer conditions further and to verify that the Mg^{2+} or aminoglycoside concentrations used in the NMR and SPR experiments do not negatively interfere with the $tRNA^{Phe}$ structure, CD experiments were performed (Figure 4). It was possible to demonstrate that neomycin B and other aminoglycosides reduced the double helical content of $tRNA^{Phe}$. This effect could be compensated for only with divalent Mg^{2+} cations, but not with monovalent Na^+. The CD experiments also showed that Mg^{2+} in general stabilized the tRNA structure. In the light of these experiments, and taking into account that high sodium chloride concentrations negatively influence signal-to-noise ratios in cryo-probe NMR experiments,[17] we used a deuterated Tris buffer with $MgCl_2$ (30 mM) for further NOE experiments with $tRNA^{Phe}$ and aminoglycosides. Working with this buffer also had the advantage that no precipitation could be observed during the subsequent NMR experiments. Although it had been reported previously that $tRNA^{Phe}$ is cleaved by aminoglycosides such as neomycin B and kanamycin A at specific sites with cleavage rates of 1–2% per hour,[18] our NMR samples containing 30 mM $MgCl_2$ and neamine, ribostamycin, or neomycin B showed negligible decomposition of $tRNA^{Phe}$ when stored after the NMR experiments at 4°C for several months. This finding is in accordance with the general stabilizing effect of Mg^{2+} seen in the CD experiments.

Being a pseudodisaccharide, neamine shows positive NOE effects in aqueous solution. All NOE effects together can only be understood if a complex mixture of conformations is assumed.[19] A sample of neamine with $tRNA^{Phe}$ displays negative NOE (Figure 5), so the NOE effects of the bound state dominate the resulting spectra. Such negative NOE effects representing the bound states of small molecules are called trNOE effects. The strong trNOE effects within the two rings (G1–G2, G2–G4, G3–G5 and S4–S2a, S5–S1, S5–S3, S6–S2a) argue strongly for the chair conformation of the two rings, shown in Schemes 1 and 2 and Figure 9, below. In these ring conformations, the hydroxy and amino functions occupy equatorial positions on the six-membered rings and are therefore energetically favored.

As shown in Figure 6, shifts of neamine resonances and, more importantly, changes in the NOE pattern suggested that a conformer selection occurs during the binding event. For bound neamine, two interglycosidic trNOE effects (G1–S4 and G1–S5) defined the RNA-bound conformation at the glycosidic linkage. The trNOE effects of G1–S6, G1–S3, and G1–G4 were just above the noise level, and trROE experiments[20] suggested these very small effects were spin diffusion. Extraction of interproton distances for $tRNA^{Phe}$-bound neamine from a trNOE

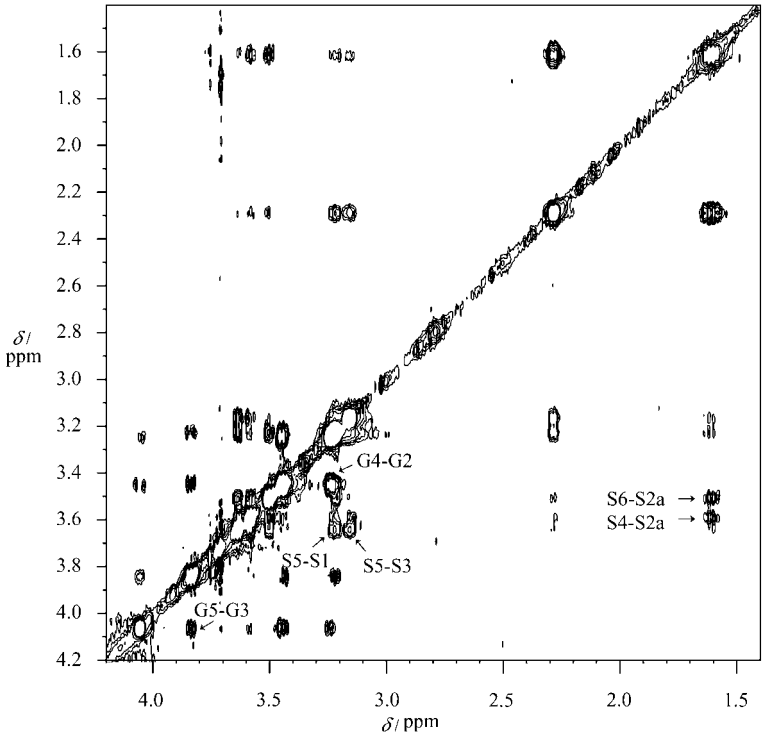

Figure 5. Section of a trNOE spectrum (700 MHz) of tRNA^{Phe}-bound neamine. TrNOE effects indicating the conformation of the two rings are pointed out.

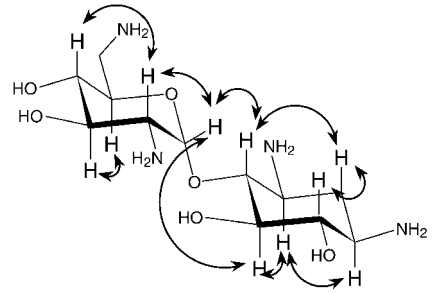

Scheme 2. Observed trNOE effects in tRNA^{Phe}-bound neamine. The strong trNOEs within the rings indicate chair conformations for the bound aminoglycoside.

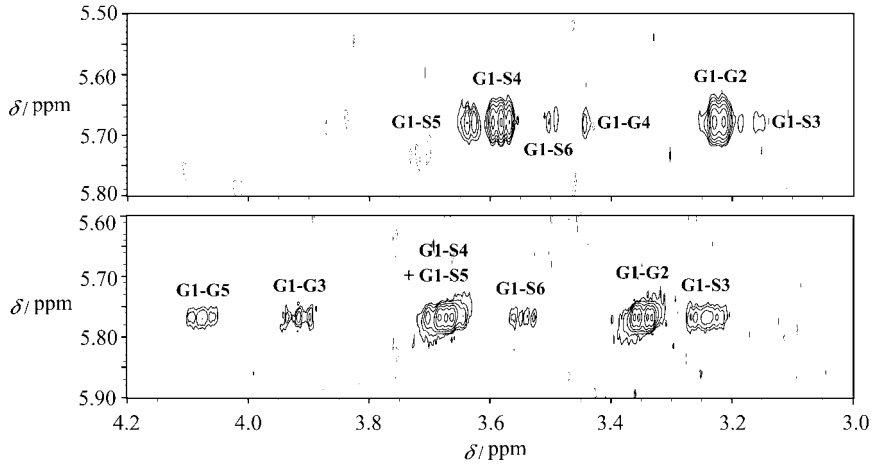

Figure 6. Sections from a NOESY spectrum of neamine (500 MHz) (bottom) and the corresponding trNOESY spectrum of the neamine–tRNA^{Phe} complex (700 MHz) (top). The G1–S3 cross peak in particular is much larger in the free state of the molecule than in the bound state; this indicates that a conformational change takes place during binding.

build-up series (Figure 7) yielded 2.4 and 3.1 Å for G1–S4 and G1–S5, respectively. With the aid of two intraglycosidic effects within the ring systems (G3–G5 and S3–S5) the experimental error for the distance determination was estimated to be smaller than 0.3 Å.

To determine the tRNA^{Phe}-bound conformation of neamine from these experimentally derived interglycosidic distances, restrained molecular dynamics (MD) simulations of neamine were performed. In these simulations the distances between G1–S4 and G1–S5 described above were used as strong restraints to define the conformational space at the glycosidic linkage in accordance with the experimental data. Figure 8 shows snapshots from such a MD simulation, displaying the torsional angles φ and ψ at the glycosidic linkage of neamine overlaid on an energy map of these two angles. The simulation populated a well defined conformational space close to a local minimum energy region around $-45°/-40°$ for φ and ψ, respectively. Neither the MD simulations nor the trNOE effects gave any indication of a different region of the aminoglycoside's conformational space being bound by tRNA^{Phe}, so it is unlikely that unspecific binding was interfering with our setup of NMR experiments. If unspecific binding were still occurring, it would have to be very minor in comparison to the specific binding observed under the conditions described here.

A final comparison of this trNOE-derived conformation of neamine with the corresponding neamine part from the crystal structure[9] is presented in Figure 9. The conformation from the middle of the populated region of Figure 8 ($\varphi/\psi = -45°/-40°$) was picked and positioned on the corresponding part of neomycin B from the crystal structure. To make comparison between the two structures easier all hydrogen atoms were omitted. It turned out that the root mean square deviation between the two structures was 0.8 Å, and thus far below the resolution of the crystal structure. As can be seen from the stereorepresentation, the atoms of the two structures have virtually the same positions within the overall shapes of the molecules. These are very important results that validate our experimental approach to the

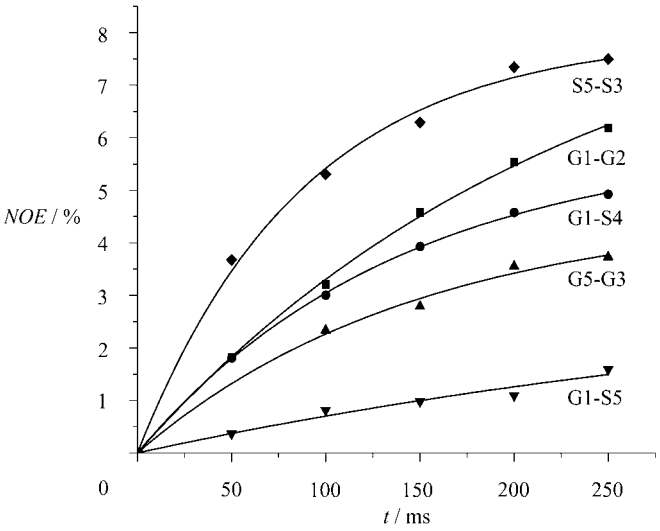

Figure 7. Build-up curves for selected trNOEs of neamine.

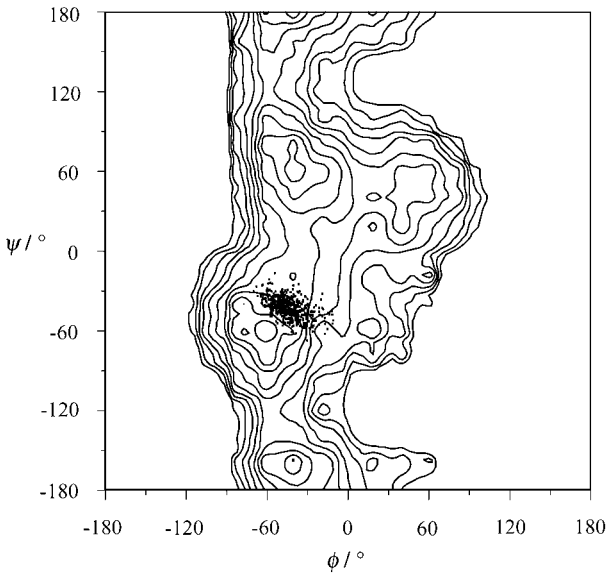

Figure 8. Potential energy surface of the α-glycosidic linkage of neamine overlaid with snapshots (dots) of a restrained MD simulation taking the determined distances for bound neamine into account.

avoidance of unspecific binding between the aminoglycoside and tRNA^{Phe} when performing NMR experiments in aqueous solution. We have thus determined the conformation of an aminoglycoside bound to a specific binding site of a RNA by trNOEs. Furthermore, we have confirmed the positions of the key polar groups of the tRNA^{Phe}-bound aminoglycoside involved in hydrogen bonds and electrostatic interaction with the RNA.

NMR experiments such as trNOE or related techniques provide additional information for the understanding of interactions on the molecular level between biomacromolecules and low-molecular-weight ligands in aqueous solution; this in turn is very helpful for the design of new lead structures. With the optimization of experimental conditions, we have successfully transferred the trNOE methodology to RNA/aminoglycoside complexes. The experimental protocol was carefully validated by using other techniques, and the buffer conditions used in this study should be generally applicable when working with RNA targets and small ligand effectors, such as aminoglycosides. Further steps of this project now include trNOE experiments with ribostamycin and neomycin B to define the bioactive conformation of the complete aminoglycoside in the tRNA^{Phe}-bound state from NMR experiments and a group epitope mapping of the interface between aminoglycosides and the RNA by STD-NMR or related techniques.[11] In this context, we are aiming to obtain more insight into the importance of the three-dimensional presentation of the hydroxy groups and the charged amino functions as well as the role of the carbohydrate backbone for the interaction of aminoglycosides with RNA.

Experimental Section

NMR spectroscopy

Sample preparation: The buffer described in the text was used for all NMR experiments. The buffer was prepared with H_2O, lyophilized, and redissolved in D_2O (pD not corrected for kinetic isotope effects). For the NOE experiments, neamine was dissolved in the buffer (25 mM in 600 μL) and this solution was lyophilized and redissolved in D_2O three times. tRNA^{Phe} from yeast (Aldrich) was first dialyzed against Millipore water to remove all salts and additives and than lyophilized. The RNA was then dissolved in deuterated buffer, and neamine was added. This solution was lyophilized and redissolved in D_2O three times. To ensure that the tRNA was correctly folded, samples were heated prior to the experiments. The final concentrations in the sample for trNOE experiments were: tRNA^{Phe} (25 μM), neamine (375 μM) (1:15).

Acquisition and processing: All NMR experiments used TSP (3-(trimethylsilyl)propionic acid) as internal reference. Experiments with free neamine were performed at 308 K on a DRX 500 spectrometer

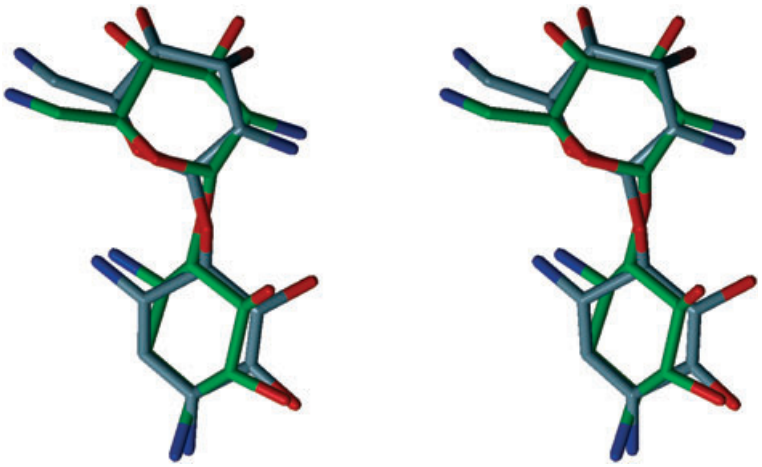

Figure 9. Stereorepresentation of a fit of the neamine part of tRNA^{Phe}-bound neomycin B from the crystal structure (gray carbon atoms) with the trNOE-derived conformation ($\varphi/\psi = 45°/40°$) of neamine (green carbon atoms). All hydrogens have been omitted.

(Bruker), experiments with the mixture of $tRNA^{Phe}$ and neamine at 308 K on a DRX 700 spectrometer (Bruker) fitted with a cryo-probe. The standard NOESY pulse sequence was used for all NOE experiments with neamine, whilst for the trNOE experiments a NOESY sequence with an additional Watergate[21] sequence for water suppression was employed. For the trROE experiment (150 ms spin lock) the standard ROESY sequence with an additional Watergate[21] sequence was used. The NOE experiment with free neamine used a 25 mM solution. The NOE experiment with neamine (800 ms mixing time) was acquired with 4096×400 data points, 32 scans and zero-filled before Fourier-transformation (apodization function squared cosine) to give a final matrix of 4096×1024 data points. TrNOE and trROE experiments were acquired with 4096×480 data points, 24 scans and zero-filled before Fourier transformation (apodization function squared cosine) to give a final matrix of 8192×1024 data points. Mixing times for the trNOE buildup series were 50, 100, 150, 200, and 250 ms. Processing was carried out with the Xwinnmr program (Bruker). The recycling delay for all NOE experiments was 3 s or longer.

Integration and distance determination: Integration of the trNOE spectra was carried out with the program Sparky.[22] The resulting data points were fitted to an exponential function of the form $f(t)=a(1-e^{-bt})$, where a and b were adjustable parameters and t the experimentally used mixing time. Initial slopes of the curves were determined from the first derivative of the function ($f(0)=a\times b$)[23] and were used to calculate the experimental interproton distances with the isolated two-spin approximation with use of the G1–G2 distance of 2.45 Å as a reference independent of the glycosidic torsion angles.

Molecular modeling and MD simulations: All calculation were performed with Sybyl (Tripos) on SGI computers using the standard Tripos force field.[24] The glycosidic torsion angles φ and ψ of neamine were defined by use of the hydrogen atoms as φ=H1G-C1G-O-C4S and ψ=C1G-O-C4S-H4S. To obtain a potential energy map of neamine a grid search calculation was performed, the glycosidic torsion angles φ and ψ being allowed to vary at 20° intervals over the complete conformational space. Isothermal contours were plotted relative to the global minimum energy conformation, defined to be at 0 kcal mol^{-1}, up to 10 kcal mol^{-1}. Restrained MD simulations of neamine started from different low energy conformations. Protonation of amino groups was followed by conjugate gradient minimization for 1000 iterations. The distance derived from trNOE experiments were used as a restraint with a force constant of 600 kcal mol^{-1} Å^{-1} and the simulations were carried out in vacuo. Equilibration was achieved by increasing the temperature from 50 K in steps of 50 K to 300 K (2 ps each). The simulation continued at a temperature parameter of 300 K for 1 ns with a step of 1 fs. Snapshots were taken after every 2 ps.

SPR experiments: SPR experiments were performed on a Biacore 3000 (Biacore) system at 20 °C. Biotinylated $tRNA^{Phe}$ was immobilized on a SA sensor chip (streptavidin immobilized on a dextran matrix). Tris buffer (20 mM Tris, 150 mM NaCl, pH 7.2, with and without 30 mM $MgCl_2$) was used. Concentrations of neomycin B ranging from 1 μM to 5 mM in buffer were injected into the flow cells and the equilibrium response was plotted against the concentration of neomycin B. Regeneration of the surface was achieved by short injections of solutions containing NaCl (1 mM) into the flow cells. Data were fitted to a binding isotherm with one or two independent binding sites.

Circular dichroism spectroscopy: To ensure that the tRNA was correctly folded, samples were heated to 85 °C for 2 min prior to each titration and equilibrated to room temperature for 5 min. CD spectra were acquired with a Jasco J-715 spectrapolarimeter fitted with a thermoelectrically controlled cell holder in the continuous wave mode. A quartz cell with a pathlength of 0.5 cm was used. Three spectra were averaged with a spectral width from 320 to 220 nm at 1 nm resolution, a time constant of 1 s, and a scan speed of 50 nm min^{-1}. Experiments were carried out with 200 μL samples (8 μM $tRNA^{Phe}$, Tris-HCl, pH 7.4) at 308 K. During the titrations reagents (aminoglycosides and salts) were added in 1 μL volumes. Following each addition of reagents, the samples were allowed to equilibrate for 5 min prior to the acquisition of the CD spectra. After baseline correction the spectra were scaled to take the dilution into account and normalized to the number of nucleotides of $tRNA^{Phe}$.

Acknowledgements

This work was supported by grants from the DFG (We 1818/4-1), the DAAD, and the Verein zur Förderung der Glycowissenschaften e.V. Prof. B. Westermann (Halle) sent us a generous gift of neamine. We wish to thank Prof. R. K. Hartmann (Marburg) for stimulating discussions about aminoglycoside binding to RNA. Profs. T. Peters (Lübeck) and B. Meyer (Hamburg) are thanked for the access to the NMR spectrometers (DFG-Project Me 1830/1-1) and the computing facilities. Prof. H. Notbohm (Lübeck) is further thanked for access to the CD spectrophotometer.

Keywords: aminoglycosides · conformation analysis · electrostatic interactions · NMR spectroscopy · tRNA

[1] a) D. J. Ecker, R. H. Griffey, *Drug Discovery Today* **1999**, *4*, 420–429; b) Y. Tor, *ChemBioChem* **2003**, *4*, 998–1007; c) G. J. Zaman, P. J. Michiels, C. A. van Boeckel, *Drug Discovery Today* **2003**, *8*, 297–306; d) Y. Thor, *ChemBioChem* **2003**, *4*, 998–1007; e) Q. Vicens, E. Westhof, *ChemBioChem* **2003**, *4*, 1018–1023.
[2] D. Moazed, H. F. Noller, *Nature* **1987**, *327*, 389–395.
[3] a) U. von Ahsen, J. Davies, R. Schroeder, *Nature* **1991**, *353*, 368–370; b) U. von Ahsen, J. Davies, R. Schroeder, *J. Mol. Biol.* **1992**, *226*, 935–941.
[4] T. K. Stage, K. J. Hertel, O. C. Uhlenbeck, *RNA* **1995**, *1*, 95–101.
[5] J. Rogers, A. H. Chang, U. von Ahsen, R. Schroeder, J. Davies, *J. Mol. Biol.* **1996**, *259*, 916–925.
[6] M. L. Zapp, S. Stern, M. R. Green, *Cell* **1993**, *74*, 969–978.
[7] H.-Y. Mei, A. A. Galan, N. S. Halim, D. P. Mack, D. W. Moreland, K. B. Sanders, H. N. Truong, A. W. Czarnik, *Bioorg. Med. Chem. Lett.* **1995**, *5*, 2755–2760.
[8] F. Walter, J. Putz, R. Giege, E. Westhof, *EMBO J.* **2002**, *21*, 760–768.
[9] N. E. Mikkelsen, K. Johansson, A. Virtanen, L. A. Kirsebom, *Nat. Struct. Biol.* **2001**, *8*, 510–514.
[10] a) T. Herrmann, E. Westhof, *Biopolymers* **1999**, *48*, 155–165; b) F. Walter, Q. Vicens, E. Westhof, *Curr. Opin. Chem. Biol.* **1999**, *3*, 694–704; c) Q. Vicens, E. Westhof, *Biopolymers* **2003**, *70*, 42–57.
[11] B. Meyer, T. Peters, *Angew. Chem.* **2003**, *115*, 890–918; *Angew. Chem. Int. Ed.* **2003**, *42*, 864–890.
[12] a) G. Bertho, P. Ladam, J. Gharbi-Benarous, M. Delaforge, J. P. Girault, *Int. J. Biol. Macromol.* **1998**, *22*, 103–127; b) G. Bertho, J. Gharbi-Benarous, M. Delaforge, J. P. Girault, *Bioorg. Med. Chem.* **1998**, *6*, 209–221; c) L. Verdier, G. Bertho, J. Gharbi-Benarous, J. P. Girault, *Bioorg. Med. Chem.* **2000**, *8*, 1225–1243; d) C. C. Zhou, S. M. Swaney, D. L. Shinabarger, B. J. Stockman, *Antimicrob. Agents Chemother.* **2002**, *46*, 625–629.
[13] a) H. Wank, R. Schroeder, *J. Mol. Biol.* **1996**, *258*, 53–61; b) C. Faber, H. Sticht, K. Schweimer, P. Rösch, *J. Biol. Chem.* **2000**, *275*, 20660–20666.
[14] a) D. E. Dorman, J. W. Paschal, K. R. Merkel, *J. Am. Chem. Soc.* **1976**, *98*, 6885–6888; b) R. E. Botto, B. Coxon, *J. Am. Chem. Soc.* **1983**, *105*, 1021–

1031; c) M. Kaul, C. M. Barbieri, J. E. Kerrigan, D. S. Pilch, *J. Mol. Biol.* **2003**, *326*, 1373 – 1387.
[15] a) G. Quingley, M. M. Teeter, A. Rich, *Proc. Natl. Acad. Sci. USA* **1978**, *75*, 64 – 68; b) B. Frydman, W. M. Westler, K. Samejima, *J. Org. Chem.* **1996**, *61*, 2588 – 2589.
[16] a) S. S. Rialdi, J. Levy, R. Bilton, *Biochemistry* **1972**, *11*, 2472 – 2479; b) R. Romer, R. Hach, *Eur. J. Biochem.* **1975**, *55*, 271 – 284; c) V. K. Misra, D. E. Draper, *J. Mol. Biol.* **2000**, *299*, 813 – 825.
[17] A. E. Kelly, H. D. Ou, R. Withers, V. Dötsch, *J. Am. Chem. Soc.* **2002**, *124*, 12013 – 12019.
[18] S. R. Kirk, Y. Tor, *Bioorg. Med. Chem.* **1999**, *7*, 1979 – 1991.
[19] J. L. Asensio, A. Hidalgo, I. Cuesta, C. Gonzalez, J. Canada, C. Vicent, J. L. Chiara, G. Cuevas, J. Jiménez-Barbero, *Chem. Eur. J.* **2002**, *8*, 5228 – 5240.
[20] T. Weimar, S. L. Harris, J. B. Pitner, K. Bock, B. M. Pinto, *Biochemistry* **1995**, *34*, 13672 – 13681.
[21] M. Piotto, V. Saudek, V. Sklenár, *J. Biomol. NMR* **1992**, *2*, 661 – 665.
[22] T. D. Goddard, D. G. Kneller, SPARKY 3, University of California, San Francisco.
[23] T. Weimar, R. Bukowski, N. M. Young, *J. Biol. Chem.* **2000**, *275*, 37006 – 37010.
[24] Sybyl molecular modeling software, version 6.7, Tripose associates, 1699 South Hanely Road, St. Louis, MO 63144-2917.

Received: October 13, 2004
Revised: March 15, 2005
Published online on June 3, 2005

